JOURNAL OF GUIDANCE, CONTROL, AND DYNAMICS
Vol. 23, No. 1, January–February 2000

Space-Based Visible Metric Accuracy

Curt von Braun,* Jayant Sharma,† and E. Michael Gaposchkin‡
Lincoln Laboratory, Massachusetts Institute of Technology, Lexington, Massachusetts 02420

In April 1996 the Midcourse Space Experiment satellite, sponsored by the Ballistic Missile Defense Organization, was launched into an 898-km altitude, nearly sun-synchronous orbit. One of the principal sensors onboard the spacecraft is the Space-Based Visible, a visible-band electrooptical camera used for space surveillance. The instrument is equipped with four adjacent 420 × 420 pixel charge-couple devices and was designed with high off-axis stray light rejection characteristics for observing near the earthlimb. As the first space-based space surveillance sensor, the Space-Based Visible's principal role is to gather metric and photometric information on a wide variety of resident space objects. To assess the metric performance of the sensor, routine on-orbit metric calibration is performed. In addition, a complete error assessment was made using actual flight data. The goal of producing 4-arc-s (1-sigma) observations of resident space objects was set during design, and early results show that this goal is being reached. The analysis of each of the error sources within the Space-Based Visible error budget is presented and results from both calibration and routine surveillance data collection events are shown. Error sources such as those associated with the sensor boresight pointing, including star catalog errors, spacecraft jitter, star centroiding, and optical distortion, along with the Midcourse Space Experiment ephemeris and the streak endpoint determination are discussed. The principal finding, as revealed through the discrepency between the theoretical error assessment and on-orbit metric calibration, spawned the identification of an unmodeled metric error source for the Space-Based Visible. With the identification and modeling of this error source, a 50% reduction in the metric error budget of the sensor is possible.

Introduction

THE Midcourse Space Experiment (MSX) is funded and managed by the Ballistic Missile Defense Organization (BMDO) with the goal of addressing fundamental phenomenological and functional issues associated with ballistic missile defense and space-based space surveillance. With its host of state-of-the-art visible-band, long-wavelength infrared and ultraviolet sensors, the spacecraft has successfully gathered high-quality data on strategic ballistic missile targets, resident space objects (RSOs), and terrestrial, earthlimb and celestial backgrounds, over a wide range of the spectrum. In addition to supporting the fundamental objectives of the BMDO, MSX has also acquired data on a variety of civilian science objectives in the areas of remote sensing, atmospheric sciences, and astronomy.

One of the principal sensors onboard MSX is the Space-Based Visible (SBV), a visible-band electro-optical camera designed to conduct technological and functional demonstrations in support of space-based space surveillance. The instrument was designed at the Massachusetts Institute of Technology Lincoln Laboratory through funding from the Space and Missile Center. As a possible flight technology demonstration for the Space-Based Infrared System-Low, the SBV represents the first space-based staring sensor for use in space surveillance. The instrument is equipped with four adjacent 420 × 420 pixel charge-couple devices (CCD) and was designed with high off-axis stray light rejection characteristics for observing near the earthlimb.

As the first space-based space surveillance sensor, SBV's principal role is to gather metric and photometric information on a wide variety of RSOs. To assess the metric performance of the sensor, routine on-orbit metric calibration is conducted. This is accomplished by observing satellites for which the positions are very well established and comparing these known positions with SBV-observed positions. During the design phase of the SBV program, the goal of producing 4-arc-s (1-sigma) metric observations of RSOs was set. This 4-arc-s error budget is composed of a wide variety of error sources, ranging from the estimated position of the sensor on-orbit to systematic uncertainties within the established star catalogs. Although on-orbit metric calibration is the only true method of determining the metric performance of the SBV, an independent error assessment was made using actual flight data. This was performed by isolating each error source within the error budget and quantifying its effect on the SBV observation.

The metric processing performed for the SBV is markedly different from that of the Ground-Based Electro-Optical Deep Space Surveillance System (GEODSS),[1,2] the optical system currently used by the U.S. Air Force for tracking RSOs. The GEODSS telescopes establish their boresight pointing through mathematical models of the telescope mount position. In contrast, the SBV matches detected star patterns and locations to star catalog positions, yielding a significantly more robust and accurate estimate than can be performed through mount modeling. One of the difficult aspects of processing space-based observations, however, is that pointing and RSO position estimates must be made in the face of spacecraft drift and jitter. Clearly, the former issue does not exist on the ground, and the latter issue is typically extremely small. Finally, as with any ground-based optical telescope or radar, it is necessary to establish the sensor's coordinates at the time an observation is taken. Whereas this can be done through a routine site survey for a ground-based instrument, it is necessary, in the case of SBV, to continuously track the MSX and estimate its on-orbit position.

This paper will present the analysis of each of the error sources within the SBV error budget and will compare the results with those established from routine calibration. Error sources such as those associated with the sensor boresight pointing, including star catalog errors, spacecraft periodic motion, star centroiding, and optical distortion, along with the MSX ephemeris and the streak endpoint determination will be discussed in detail. Finally, some conclusions will be drawn regarding the overall metric performance of the SBV and its impact on space surveillance.

SBV Data Processing

The SBV performs data collection in, most commonly, a staring mode. In this mode, light from stellar sources, the cosmic background and any diffuse or specular reflection of an RSO within the field of view (FOV) will be detected on the focal plane. The light is gathered on the detector for integration periods of 0.4, 0.625, 1.0,

Received 16 November 1998; revision received 20 July 1999; accepted for publication 3 August 1999. This material is declared a work of the U.S. Government and is not subject to copyright protection in the United States.

*Assistant Group Leader and Midcourse Space Experiment Surveillance Principal Investigator.

†Technical Staff Member, Surveillance Techniques.

‡Senior Staff Member (retired) and former Midcourse Space Experiment Surveillance Principal Investigator.

Fig. 1 SBV image of LAGEOS.

and 1.6 s, depending on the operating type of data collection. An image gathered over one integration period is referred to as a frame. One raw or unprocessed frame of SBV data appears as a star field on a dark background and, if an RSO is in the FOV, a short streak of illuminated pixels. Typically, a streak taken over one frame is not long enough to distinguish it from a stellar point source. As a consequence, it is necessary to superimpose multiple frames to produce an image that can be effectively processed. A collection of these images, namely, a frameset, typically consists of between 8 and 16 frames. Figure 1 shows an SBV image of the Laser Geodynamics Satellite (LAGEOS) with a 16-frame frameset with an integration period of 1.0 s.

The process of establishing an observation (right ascension and declination) of an RSO entails, first, determining the precise pointing of the boresight of the sensor in an inertial frame, then determining the position of the beginning and endpoints of that streak on the focal plane. Once these focal-plane positions are known, they can then be transformed into right ascension and declination. Finally, the position of the observing platform must be established to support the angular measurements. For a detailed discussion of the processing of SBV image data, the reader is referred to Ref. 3.

Once the observations of an RSO are established, they must be qualified through calibration. This is conducted routinely in operations, and the data are compiled and compared with the independently determined error budget. Metric calibration is performed by observing satellites for which the positions are known to a very high accuracy. These satellites, herein referred to as calibration objects, are tracked using high-precision laser ranging observations. These laser data, along with ground radar measurements, are used to establish the satellites' positions to better than about 10 cm. By tracking these objects using SBV, it is then possible to calibrate the metric observations using the known positions and to isolate those errors caused by the SBV sensor. Now a detailed discussion of each of the known error sources will be presented.

SBV Error Budget

MSX Ephemeris and Timing

As already mentioned, observations of an RSO from a moving space platform would be incomplete if they were not accompanied by information regarding the location of the sensor in space, SBV in this case, during the data collection. As a consequence, it is necessary to supplement the reduced right ascension and declination observations of a target with the ephemeris of the MSX.

As part of the Surveillance Data Analysis Center (SDAC) at Lincoln Laboratory, the orbital position of MSX has been produced every day since launch. This is performed using the space ground link system (SGLS), a global network of tracking stations used by the U.S. Air Force for tracking a large number of its satellites. The principles underlying the modeling and routine processing of the tracking data of MSX are beyond the scope of this paper; detailed explanations may be found in Refs. 4 and 5.

The contribution of the error of the position of MSX to the SBV error budget is a function of the range to the RSO. For example, a target at a range of 3000 km produces a 1-arc-s error in the SBV observation, if the uncertainty in the position of MSX is limited to 15 m. In contrast, an RSO in geosynchronous orbit at a range of 42,000 km produces an error in the SBV observation of just 0.07 arc-s. Given that ranges of only 3000 km are uncommon during operations and that 1 arc-s is limited to 25% of the total SBV error budget, the goal of routinely producing a 15-m orbit for MSX was set during design. This goal has, in fact, been exceeded, with orbit position uncertainties averaging the 8-m level, as reported in Ref. 4. As a consequence, the contribution of the error in the MSX position to an SBV observation is typically less than 0.5 arc-s and, for geosynchronous objects, is essentially negligible. Note that for near real-time (less than 24 h) ground processing of SBV data within the Space Surveillance Network (SSN), postfit orbits of MSX are not possible, and errors in the predicted MSX position may be as large as 25 m. This is not a concern for deep space objects but could be an issue for RSOs at close range.

Uncertainties in the onboard system clocks used to tag SBV observations also contribute to the SBV error budget. The MSX system requirements, established independently from those of SBV, placed the specification of 1 ms on the system clocks. Because timing errors are a function of range to the RSO and the relative motion of the RSO across the SBV focal plane, it is possible to set reasonable bounds on the errors. In a worst-case scenario, such as observing a target at 2500 km when the relative velocity is at its maximum of 15 km/s, a 1-ms timing error produces a 1.3-arc-s error in the SBV observation. In contrast, a best-case scenario entails observing a geosynchronous belt satellite while MSX crosses over one of the poles, giving a relative velocity of 3.1 km/s (absolute velocity of the target only). This situation produces an error of about 0.02 arc-s. Conseqently, timing errors are typically less than 1 arc-s and are frequently completely negligible.

Boresight Pointing

To determine the boresight pointing of the SBV, it is necessary to match the collection of star detections on the focal plane with cataloged star positions. In matching these positions in a least-squares sense, a correction to the a priori boresight pointing is determined. The product of this process will be a set of star-match residuals that as an ensemble quantify the ability to match an average star. The formal uncertainty of the boresight pointing can then be determined based on this information, in addition to the number of stars matched in a given FOV. It is this stage of SBV data reduction that introduces some of the most subtle and important errors in the process. Errors associated with the star catalogs, the algorithms used for centroiding the star detections on the focal plane, the distortion of the CCD image introduced by the optics, and the actual spacecraft attitude drift and periodic motion all contribute to the boresight pointing error. A discussion of each of these error sources follows.

Star Catalogs

During routine processing of the SBV data, "The Astrographic Catalogue of Reference Stars (ACRS)"[6] is most commonly used. This catalog, compiled at the U.S. Naval Observatory, contains approximately 320,000 stars with visual magnitudes of 10.5 and brighter. In addition to this catalog, the SDAC uses the Hubble "Guide Star Catalogue" (GSC) that was constructed to support the Hubble Space Telescope during operations.[7] The GSC contains more than 15×10^6 stars with visual magnitudes of 16 and brighter. Table 1 shows the various characteristics of each catalog.

With regard to the discussion of the SBV error budget, the random and systematic errors are of critical importance. Although the GSC offers a far denser array of stars per square degree than does the ACRS, the systematic errors are larger. In fact, as will be illustrated in following section, it is the systematic errors in the ACRS that are limiting the boresight pointing for SBV.

Table 1 Star catalogs used with SBV

Star catalog	Affiliation	No. of stars	Limiting magnitude	Average no. of stars per square degree	Systematic errors (arc-s)	Random errors (arc-s)
ACRS	U.S. Naval Observatory	3.2×10^5	10.5	7.9	0.1–0.2	0.25–1.0
GSC	Hubble Space Telescope Institute	15×10^6	16	365	0.4–1.6	0.3–0.8

Star Centroiding

A study of the errors due to the centroiding of the group of illuminated pixels composing a star detection was conducted prior to launch. These results found that the performance of the centroiding algorithm decreased as the signal-to-noiseratio of the star detection on the focal plane decreased. From a Monte Carlo simulation of the errors as a function of detected magnitude, it was found that for a star of 10th magnitude, the centroiding errors were limited to 0.1 arc-s. Similarly, for stars as dim as 14th magnitude, centroiding errors rose to as large as 6.6 arc-s. As a consequence of this study, the star matching process is typically limited to stars of 12th or 13th magnitude or brighter.

In the sections that follow, it will be discussed how centroiding error is affected by spacecraft attitude drift and periodic motion and what influence they have on the overall boresight pointing error.

Spacecraft Attitude Drift and Periodic Motion

Although spacecraft attitude drift and periodic motion do not currently factor directly into the SBV error budget, they do influence the ability to perform centroiding on the star detection. While the sensor is gathering light during one integration period, or exposure, the spacecraft attitude is experiencing some degree of secular and periodic motion. The secular behavior causes the grouping of illuminated pixels from a detection to elongate in the direction of the drift motion. This effect, if substantial, shifts the location of the centroid, when compared to one determined when drift is not present. Similarly, the periodic motion tends to create an enlargement or blurring of the group that affects the centroid location. Although neither of these effects is large, they both degrade the quality of the star-fit residuals.

During a pointing alignment event on the MSX, the SBV produces an image every 1.0 s. As mentioned earlier, these frames are routinely processed in batches of between 8 and 16. However, if each frame, individually, is matched to the star catalog, the corrected pointing can be determined every 1.0 s. This, effectively, produces a time series of the attitude of the spacecraft, identifying both the drift and the periodic motion, as sampled at 1 Hz. Note that periodic motion at frequencies both higher and lower than 1 Hz do exist, but only effects at frequencies of 1 Hz and lower can be identified using SBV.

This process was carried out using 10 framesets from five different MSX pointing alignment events conducted over the first six months of the mission. From these, an average value for the drift and 1-Hz periodic motion was determined. Figure 2a shows a typical time series of the difference of the right ascension (RA), declination (DEC), and roll (ROLL) from the boresight pointing of the initial frame for a 16-frame frameset. Figure 2b effectively removes the drift effect by differencing the pointing results for a given frame with those of the previous frame. This allows for the assessment of the 1-Hz periodic motion.

For the pointing alignment data analyzed, the drift varied between 0 and 0.3 arc-s/s, in absolute value, and the average standard deviation of the 1-Hz periodic motion in RA and DEC was 0.4 arc-s. Given that these quantities only indirectly contribute to the error budget by degrading the centroiding, these values will not adversely affect the boresight pointing. Note that, although the roll angle appears to vary to a much larger degree than do the RA and DEC, this is only an artifact of the poor sensitivity of SBV to this direction of motion and should not be concluded as the actual roll behavior.

Optical Distortion

To produce boresight pointing results to the level of 1 arc-s, it is necessary to model the optical distortion of the camera. Predominantly for the purposes of reducing stray light from the earthlimb, hyperbolic and elliptic mirrors are used by the SBV to project the incoming light onto the focal plane. These mirrors produce an image that is distorted, and this distortion must be accounted for during the star matching process. Note that this distortion is severe enough, particularly at the outer edges of the CCD array, to shift the position of a star or RSO detection by as much as 100 pixels.

During the first few months of the mission, a rigorous determination of the distortion model was conducted using actual flight data. The primary requirements of this mathematical distortion map are that it be valid over the entire CCD, that it be stable over time, and that the remaining unmodeled distortion errors not be so large as to produce boresight pointing results poorer than 1 arc-s. As a consequence, the MSX pointing alignment events, which are staring events at fields rich in stars, were used for this purpose. To achieve a model that is valid over the entire array, it was necessary to have a large number of stars detected everywhere on the focal plane. This allowed for the accurate determination of the map.

The process of matching the distorted detected star positions to the actual catalog star positions is performed in focal plane coordinates. As a consequence, the star positions are mapped onto the array by first translating and rotating the cataloged star field and aligning it with the detected field. Then the distortion map is used to project these translated/rotated cataloged positions onto the distorted focal plane image. Once this is complete, the star matching is performed in a least-squares sense and the residuals are determined.

The mathematical structure of the distortion map consists of the translation, referred to as the boresight offset (z_o, y_o), followed by a rotation about the roll axis by the error in the roll angle θ, such that

$$\begin{bmatrix} \xi \\ \eta \end{bmatrix} = R(\theta) \begin{bmatrix} z - z_o \\ y - y_o \end{bmatrix}$$

where

$$R = \begin{bmatrix} \cos(\theta) & \sin(\theta) \\ -\sin(\theta) & \cos(\theta) \end{bmatrix}$$

This produces the coordinate pair ξ and η that represents the undistorted cataloged star positions on the focal plane. These coordinates are then transformed into distorted coordinates z' and y', such that

$$\begin{bmatrix} z' \\ y' \end{bmatrix} = A \begin{bmatrix} \xi \\ \eta \end{bmatrix}$$

where

$$A = \begin{bmatrix} a_{11} & a_{12} \\ a_{21} & a_{22} \end{bmatrix}$$

and

$$a_{11} = a_{11}^{00} + a_{11}^{10}\xi + a_{11}^{01}\eta + a_{11}^{20}\xi^2 + a_{11}^{11}\xi\eta + a_{11}^{02}\eta^2$$

$$a_{21} = a_{21}^{00} + a_{21}^{10}\xi + a_{21}^{01}\eta + a_{21}^{20}\xi^2 + a_{21}^{11}\xi\eta + a_{21}^{02}\eta^2$$

$$a_{12} = a_{21}, \qquad a_{22} = a_{22}^{00} + a_{22}^{10}\xi + a_{22}^{01}\eta + a_{22}^{20}\xi^2 + a_{22}^{11}\xi\eta + a_{22}^{02}\eta^2$$

For the determination of the distortion map, it was necessary to simultaneously estimate the boresight offset, the error in roll, and each of the 18 distortion coefficients during the star matching procedure. This was performed for each of the four CCDs using 36 framesets from five pointing alignment events (DC-29) and one SBV calibration event (SU-03). Because of the large number of stars needed for the determination of the map, the GSC was used. Figure 3 shows a typical pointing alignment star field and the stars that were matched

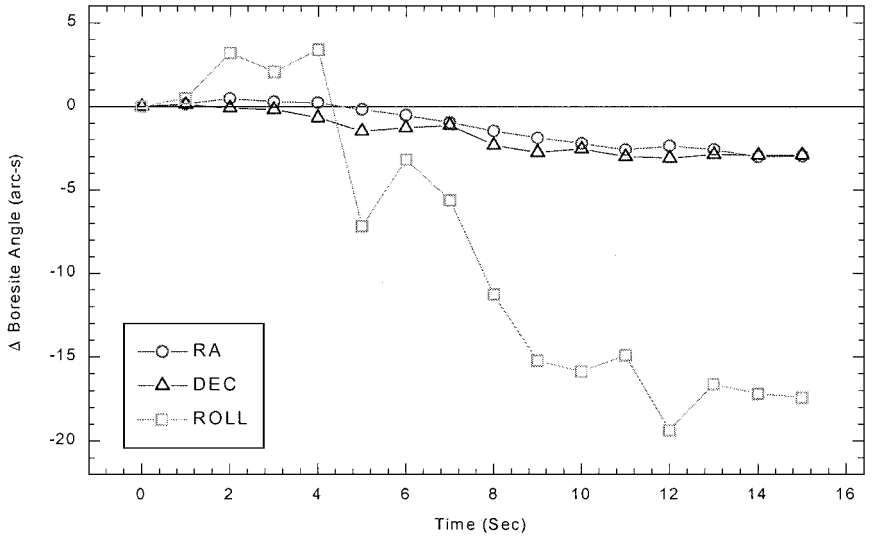

Fig. 2a Spacecraft drift.

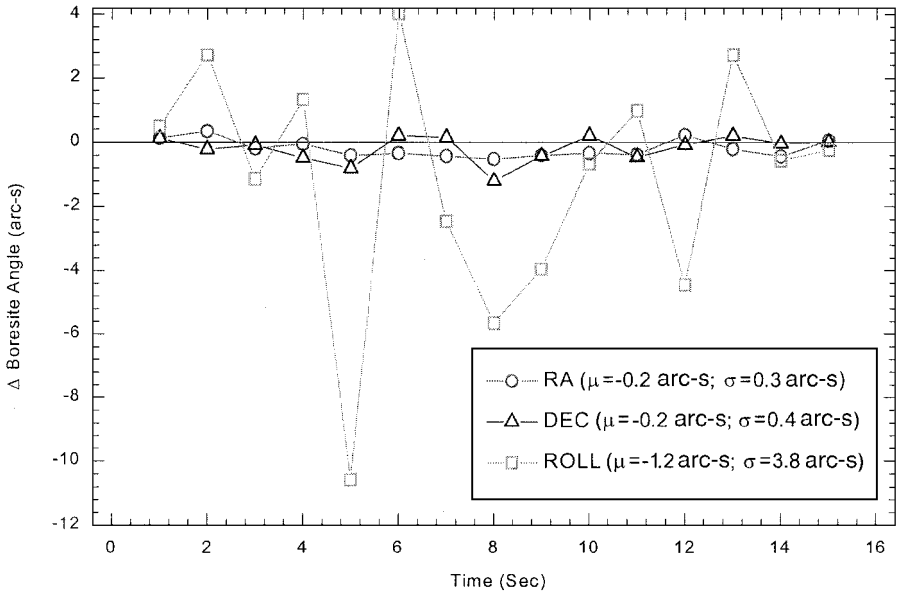

Fig. 2b Spacecraft periodic motion, 1 Hz.

Fig. 3a MSX/SBV pointing alignment star field.

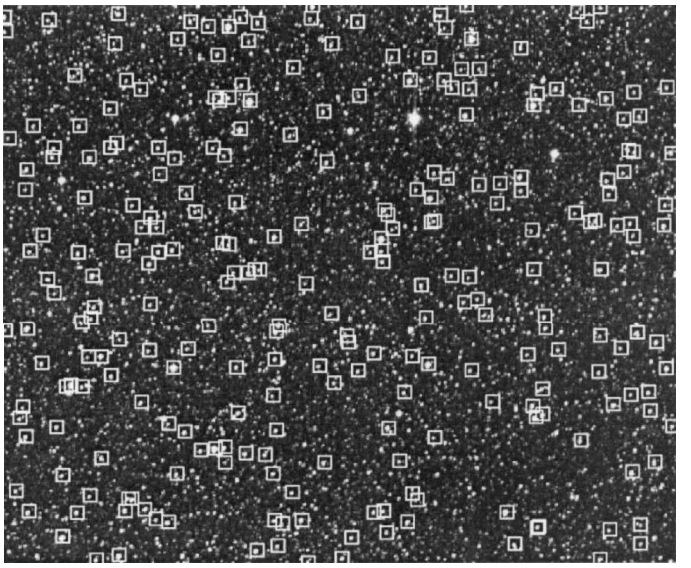

Fig. 3b Star matched during alignment event, indicated by box.

Table 2 Star match quality in distortion map study

CCD	No. of framesets	rms Star fit, arc-s
1	6	0.8
2	9	1.0
3	13	0.9
3	9	0.9

Table 3 Determination of offsets and roll error

Event	CCD	$\langle z_o \rangle$, pixels	σ_{zo}, pixels	$\langle y_o \rangle$, pixels	σ_{yo}, pixels	$\langle \theta \rangle$, deg	σ_θ, deg
DC-29	1	974.50	0.66	2.85	0.21	−0.610	0.005
DC-29	2	500.80	0.76	−11.88	0.18	−0.493	0.006
DC-29	3	17.66	0.66	−7.87	0.16	−0.383	0.009
SU-03	3	18.74	0.47	−9.05	0.12	−0.378	0.009
DC-29	4	−455.54	0.77	14.87	0.24	−0.277	0.007

in the least-squares process. In this particular case, over 290 stars were correlated to the catalog. Table 2 shows the quality of the residuals of the least-squares star matching procedure, and Table 3 shows the estimated values for the offset, the error in roll, and their formal estimated uncertainties. It was found that, although it was clearly necessary to estimate all 18 coefficients in the distortion map during its development, for routine operations it is sufficient to estimate the boresight offset, the error in roll, and only the two most important terms in the distortion map, a_{11}^{00} and a_{22}^{00}. These coefficients represent the zeroth-order distortion or stretching along the z and y coordinates.

Boresight Pointing Results

Having identified the various error sources involved in determining the boresight pointing, it is now possible to get an estimate of the total contribution that pointing makes to the 4-arc-s performance goal for SBV. As discussed, the pointing error budget is made up of star catalog error, spacecraft attitude drift and jitter, centroiding error, and optical distortion. These errors, however, do not simply superpose to yield the total pointing error; they merely act to produce the residual error, when star detections are matched to a catalog.

The formal uncertainty in pointing is, essentially, based on the average star-fit quality, an example of which is shown in Table 2, and the total number of stars matched in a given frameset. If there were no systematic errors present in the star catalog and the errors in pointing and roll were not correlated with each other, the formal error covariance would be a diagonal matrix. In such a case, the error in each of the two pointing variables (RA and DEC) would be simply the star-fit residual reduced by $\sqrt{n}$, where n is the number of matched stars. With star matches of between 10 and 500 stars, depending on the star field and star catalog used, this would produce a boresight pointing uncertainty of between 0.3 and 0.05 arc-s, respectively. It, however, is not possible to determine pointing to these lowest levels because the ACRS star catalog has systematic errors of 0.1–0.2 arc-s and the GSC has errors between 0.4 and 1.6 arc-s.

This limitation in boresight pointing due to systematic errors in the star catalogs is evident from all of the SBV data gathered since launch. Routine processing of SBV data uses the ACRS and matches, on average, 11 stars per frameset, with an average rms residual of 0.8 arc-s (Ref. 3). As a consequence, the pointing uncertainty of SBV is limited by the current star catalog systematic errors. This limitation exists because the estimate of the pointing error will be approximately a factor of three less than the rms residual, due to the number of stars matched. Note that the small average number of star matches, given the dense field of stars often available, is due to a deliberate thresholding of the dimmest stars and to the use of the ACRS, which offers only about eight stars per square degree.

Streak Endpoint Determination

The last and, currently, the largest error source in the SBV observation budget is that created during the determination of the beginning and endpoints of an RSO streak passing through the focal plane (Fig. 1). Streak endpoint determination is performed either onboard or on the ground, and processed using a least-squares technique. The algorithm gathers a 5-pixel-wide swath of data comprising the streak and performs a best fit of a line to the data. The linear assumption of the streak is well supported for the integration periods of the sensor and the rate of motion of RSOs across the CCD. For a more detailed explanation of the process of determining the endpoints in focal plane coordinates and how these are then transformed to RA and DEC, the reader is referred to Ref. 3.

Table 4 Star match quality for SEP determination

Frameset no.	Matches/streaks	rms Star fit,[a] arc-s
11,163	29/30	1.2
11,167	22/23	1.3
11,169	29/30	1.5
11,170	20/21	1.0
11,173	27/28	0.9

[a] Average 1.2.

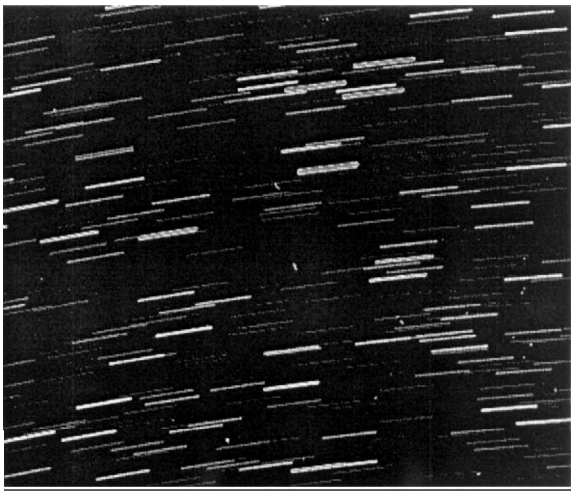

Fig. 4 Ephemeris track data collection.

The assessment of the quality of streak endpoint determination was performed by evaluating the ability to match stars to the catalog in a mode of tracking referred to as ephemeris tracking. As already mentioned, the normal mode of data collection with SBV is a staring mode that produces an image as shown in Fig. 1. However, SBV is also able to track a target, such that the object stays fixed in the center of the focal plane. In this way, the object will appear as a centralized grouping of illuminated pixels, while the stars will streak across the focal plane. Figure 4 shows a typical image from an ephemeris track data collection event. It can be seen that the stars appear as uniform lines of comparable lengths. By using the ephemeris track mode of data collection, it is possible to match the beginning and end of each of the streaks on the focal plane to stars in the catalog. Through the determination of this rms fit over the entire CCD and over a number of data sets, an overall assessment of the performance of the algorithm can be made.

A study was made using five framesets of ephemeris track data of the Lincoln Experimental Satellite 8 within the first few months of the MSX mission. For the dataset shown in Fig. 4, with star detections dimmer than 14th visual magnitude thresholded out, 28 detected streaks were matched to 27 cataloged stars to an rms fit quality of 0.9 arc-s. Table 4 shows the results from the four other framesets, giving an average rms fit of 1.2 arc-s. It was expected that the process of matching stars during an ephemeris track data collection would not perform as well as during a staring mode. This is because it is, fundamentally, more challenging to perform accurate metric detection and processing while the vehicle is slewing than while the vehicle is stabilized. By comparing the results from Table 2 with those of Table 4, it can be seen that there was a 20–30% degradation in the quality of the matches.

One important characteristic that the streak endpoint determination algorithm has is that it be robust across a wide range of visual magnitudes. This would allow for the observation of RSOs ranging from as bright as 6th magnitude, possible during high specular periods, to as dim as 14th magnitude, for small or highly emissive objects. This was assessed by investigating the quality of the endpoint determinations as a function of magnitude. Figure 5 shows both the individual endpoint focal plane coordinate star-fit residuals and the overall rms of the fit to the endpoints as a function of SBV magnitude. It is clear from these results that the algorithm performance is quite robust over the desired range.

Given these results, it seems that both the quality of the streak endpoint determination algorithm and the robustness of its performance across visual/SBV magnitude are sufficient to meet the total 4-arc-s goal for SBV observations.

Prelaunch Budget Assessment

Prior to the launch of SBV, a complete error determination was made based on observations taken by an SBV-grade CCD located at the Lincoln Laboratory Experimental Test Site (ETS) in Socorro, New Mexico in 1991. Observations of a variety of RSOs were gathered for the purposes of testing hardware and software and for error assessment. From these data, a rigorous study, using the techniques described earlier, was performed. The overall results of this work are shown in Table 5.

A few comments should be made on the determination of this error budget. It is clear that, prior to launch, it was not possible to assess the actual MSX ephemeris error. However, simulations had shown that it would be possible to meet the 15-m position goal.[5] As a consequence, a contribution of 15 m in ephemeris error was used in the error budget. A similar approach was taken for the satellite clock timing errors: the spacecraft specification of 1 ms was used. Finally, during the ETS observations using the SBV-quality CCD, no optical distortion was present. As mentioned earlier, the distortion exists due to the presence of the elliptic and hyperbolic mirrors in the optical path of the SBV. Because only the CCD and not the entire telescope was taken to ETS, distortion was absent from the data. An independent simulation of the distortion placed the error at 1.5 arc-s, but this would be incorporated in the boresight error.

The total SBV error budget is determined by assuming that the error sources due to the MSX ephemeris, the satellite clock used for tagging the observations, the determination of the sensor boresight, and the determination of the streak endpoints (SEP) are independent. As elaborated on earlier, errors due to the star catalogs, centroiding, spacecraft attitude drift and periodic motion, and optical distortion all exist but as part of the boresight pointing error. With the assumption of independence, the total error can be expressed by

$$\sigma^2 = \sigma^2_{\text{ephemeris}} + \sigma^2_{\text{timing}} + \sigma^2_{\text{boresight}} + \sigma^2_{\text{SEP}} + \sigma^2_{\text{unknown}}$$

where the errors due to unknowns have yet to be established.

Table 5 SBV prelaunch error budget

Error source	Nominal (arc-s)
Ephemeris, 15 m	1.0
Timing, 1 ms	0.6
Boresight pointing[a]	1.0[b]
Distortion[c]	1.5
SEP[a]	1.8
Total RSS error	2.8

[a] Based on actual ETS CCD observations.
[b] Star catalog (ACRS), with random and systematics errors; star centroiding; and periodic motion.
[c] No distortion present in ETS data.

On-Orbit Budget Assessment

In much the same way as described earlier, the actual error budget for SBV was determined. It can be seen in Table 6 that there are a number of improvements from the budget shown in Table 5. The first improvement is with respect to the MSX ephemeris. For the on-orbit assessment, actual MSX positions are known.[4] Estimation of the position of MSX is routinely at the 8-m level, thus giving almost a 50% reduction from prelaunch levels, in the errors due to this source. The other significant difference in the prelaunch and on-orbit error assessments is in the boresight pointing. Prior to launch it was expected that distortion would be a limiting error in the determination of the boresight. However, due primarily to a redesign of the distortion model in the early part of the mission and to a number of software enhancements since launch, the boresight pointing is now limited by the quality of the star catalogs and contributes only modestly to the overall error budget.

It seems from these results that RSO observations using SBV are available at the 2-arc-s level, a reduction of 50% over the 4-arc-s goal set during design. However, it is only possible to verify this finding through on-orbit metric calibration.

SBV Metric Calibration

Whereas an independent assessment of the SBV errors is of tremendous value to understanding the sensor's performance, the only true test of the quality of the observations is through routine calibration using known references. This is performed routinely on-orbit using calibration objects. Typically, SBV operations uses LAGEOS II as its calibration object, although other objects such as LAGEOS I, AJASI and Starlette have been tracked. In addition, it has been found that the constellation of GLONASS satellites has proven to be an extremely reliable calibration target, due primarily

Table 6 SBV postlaunch error budget

Error source	Nominal (arc-s)
Ephemeris, 15 m	1.0
Timing, 1 ms[a]	0.6
Boresight pointing[b]	0.2[c]
SEP[b]	1.2
Total RSS error	1.7

[a] Assume specification achieved.
[b] Distortion included.
[c] Star catalog (ACRS), with random and systematics errors; star centroiding; and periodic motion.

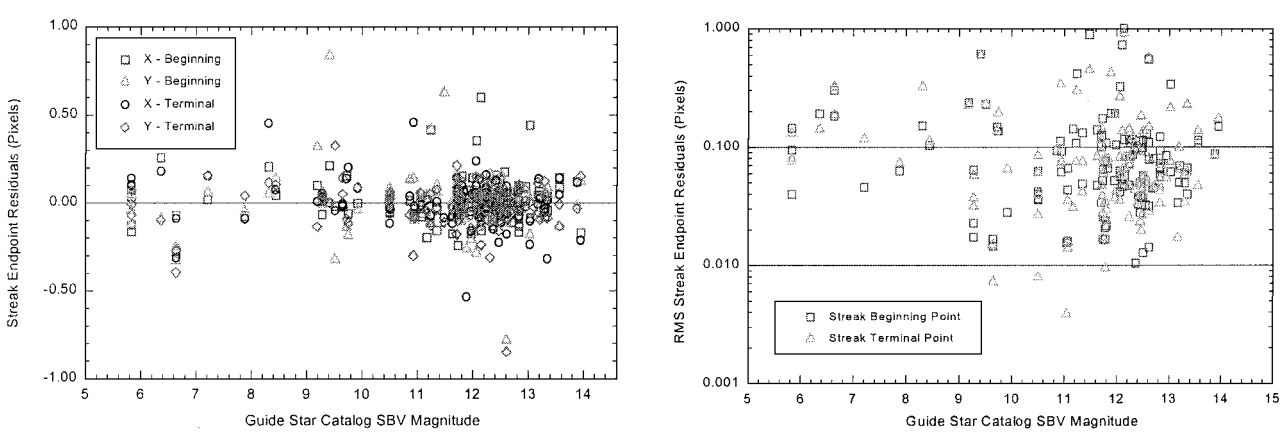

Fig. 5 Streak magnitude dependence; 1 pixel = 12.1 arc-s.

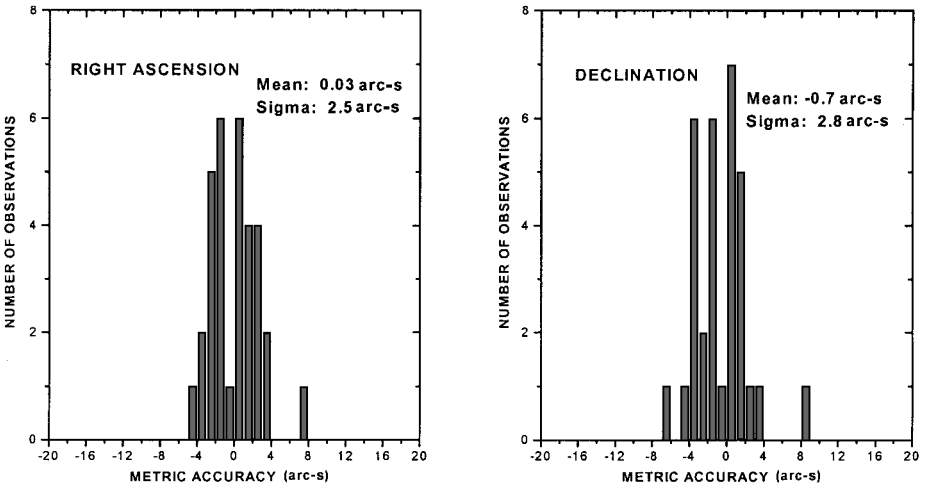

Fig. 6 GLONASS (23511) residuals from SBV.

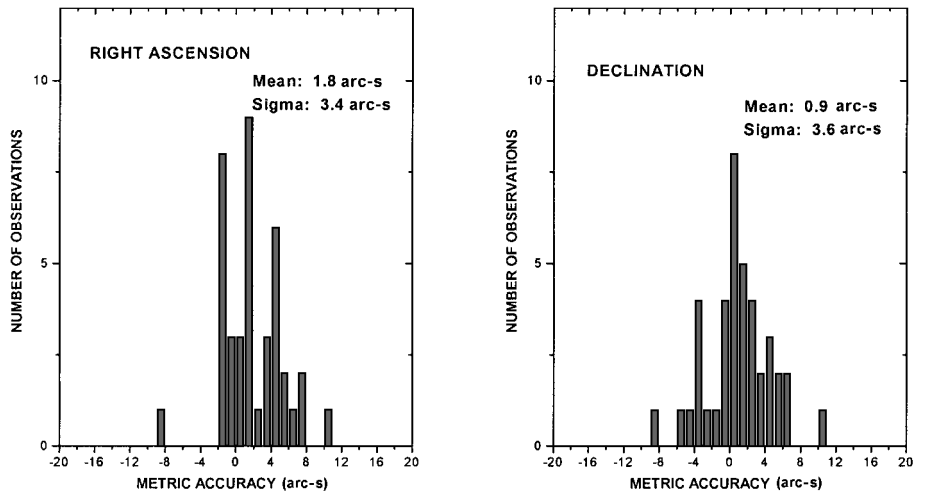

Fig. 7 LAGEOS II (22195) residuals from SBV.

to the rich supply of ground observations from the SSN network that are needed to produce a reference position. Through the use of LAGEOS II and a variety of GLONASS satellites, it has been possible to establish the current performance of SBV. Figure 6 shows the current metric performance of SBV with GLONASS (23511) data gathered currently. It is clear that the quality of the residuals is at the 4-arc-s level but is not at the level of the independent error assessment. There are several possible explanations for this discrepancy. First, at the time these data were analyzed, the precise ephemeris of MSX was not available. All of these data were processed using predicted positions of the satellite and are likely to have errors at the 25-m level. This could degrade the quality of the observation by as much as 1 arc-s. In addition, corrections to the clock, updates to the telemetry stream correcting for biases and drifts in the satellite clock, were also not applied to these data. These corrections, although different from the timing errors discussed earlier, could lead to errors at least as large in magnitude to those already in the error budget.

In a similar way, Fig. 7 shows residuals of observations of LAGEOS II with known positions on orbit. These results show, to a larger degree than with GLONASS, the issues of using a predicted ephemeris instead of a precise position estimate and the effect of the clock corrections. Both of these errors are larger for LAGEOS II than for GLONASS because of the range to these satellites. GLONASS (SSN 23511) is in a semisynchronous orbit at 19,070 km in altitude and LAGEOS II is in 5780-km-altitude orbit. Both the ephemeris error and the clock correction problem are reduced as the range to the target increases. As a consequence, for objects at close range, both of these error sources can become substantial. It is felt that, when these data are reprocessed using updated ephemeris and clock correction information, the results of the LAGEOS II observations will be reduced by as much as 20%, whereas the GLONASS residuals will likely reduce by somewhat less.

Conclusions

The work presented has shown that, while the goal of producing 4-arc-s observations of resident space objects using the SBV camera has been reached, a discrepency between the theoretical error budget and the on-orbit calibration revealed that future improvements to the metric performance of the sensor could be made. The independent error assessment indicated that observations to the 2-arc-s level were possible, through the identification and modeling of the metric error source causing the discrepency. In fact, the unmodeled source was identified and is the topic of an accompanying paper in this issue.

References

[1]Beatty, J. K., "The GEODSS Difference," *Sky and Telescope*, Vol. 63, No. 5, 1982, pp. 469–473.

[2]Pearce, E., "Electro-Optical Deep Space Tracking," *Proceedings of the Third US/Russian Space Surveillance Workshop*, U.S. Naval Observatory, Washington, DC, 1998, pp. 15–25.

[3]Sharma, J., von Braun, C., and Gaposchkin, E. M., "Space-Based Visible Data Reduction," *Journal of Guidance, Control, and Dynamics*, Vol. 23, No. 1, 2000, pp. 171–175.

[4]Abbot, R. I., Gaposchkin, E. M., and von Braun, C., "Midcourse Space Experiment Precision Ephemeris," *Journal of Guidance, Control, and Dynamics*, Vol. 23, No. 1, 2000, pp. 187–191.

[5]von Braun, C., "Cryogen Thrust Modeling for MSX Ephemeris Generation," AIAA Paper 96-121, Feb. 1996.

[6]Corbin, T. E., and Urban, S. E., "The Astrographic Catalogue of Reference Stars (ACRS)," *Mapping the Sky*, International Astronomical Union Symposium 133, Kluwer Academic, Norwell, MA, 1988, p. 287.

[7]Lasker, B. M., Sturch, C. R., McLean, B. J., et al., "Guide Star Catalogue," *Astronomical Journal*, Vol. 99, No. 6, 1990, pp. 2019–2058.